

Supplementary Information

**Contaminant bioaccessibility in abandoned mine tailings in Namibia changes along a climatic gradient**

Vojtěch Ettler<sup>1\*</sup>, Tereza Křížová<sup>1</sup>, Martin Mihaljevič<sup>1</sup>, Petr Drahota<sup>1</sup>,  
Martin Racek<sup>2</sup>, Bohdan Kříbek<sup>3</sup>, Aleš Vaněk<sup>4</sup>, Vít Penížek<sup>4</sup>, Tereza Zádorová<sup>4</sup>,  
Ondra Sracek<sup>5</sup> & Ben Mapani<sup>6</sup>

1. Institute of Geochemistry, Mineralogy and Mineral Resources, Faculty of Science, Charles University, Albertov 6, 128 00 Prague 2, Czech Republic (\*corresponding author, E-mail: ettler@natur.cuni.cz)
2. Institute of Petrology and Structure Geology, Faculty of Science, Charles University, Albertov 6, 128 00 Prague 2, Czech Republic
3. Czech Geological Survey, Geologická 6, 152 00 Prague 5, Czech Republic
4. Department of Soil Science and Soil Protection, Faculty of Agrobiology, Food and Natural Resources, Czech University of Life Sciences Prague, Kamýcká 129, 165 00 Prague 6, Czech Republic
5. Department of Geology, Faculty of Science, Palacký University in Olomouc, 17. listopadu 12, 771 46 Olomouc, Czech Republic
6. Department of Civil, Mining and Process Engineering, Namibia University of Science and Technology, Windhoek, Namibia

**Contains: 1 text, 9 tables and 7 figures**

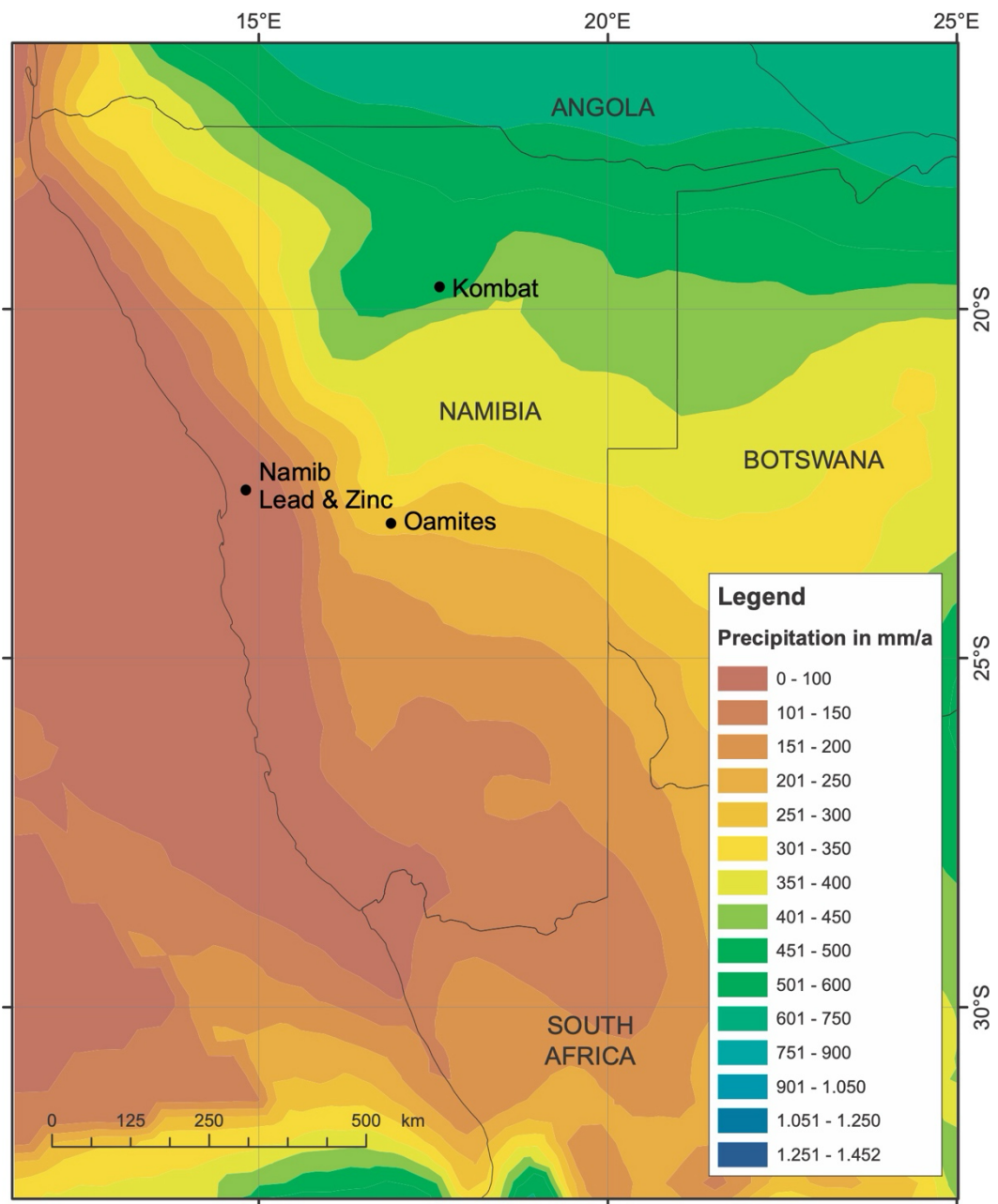


**Figure S1.** Map of long-term annual precipitation in Namibia with the indication of Kombat, Oamites, and Namib Lead & Zinc sites (data from New et al., 1999<sup>1</sup>; map downloaded from F1 project site<sup>2</sup>: <https://www.uni-koeln.de/sfb389/e/e1/index.htm>).

## Description, history, and previous investigations of the studied mining sites

**Kombat** is situated in the Otavi Mountainland in the Otjozondjupa region in northeastern Namibia. The carbonate-hosted Cu-Pb-Zn-Ag mineralization was exploited mainly between 1962 and 2008, when the mine was closed due to flooding. During this period, 12.46 million tonnes of ore with an average Cu grade of 2.6% was mined ([trigonmetals.com/kombat-mine](http://trigonmetals.com/kombat-mine)).<sup>3</sup> More than 300 Mt of tailings was deposited on the tailings dam near the village and farmlands. More detailed information about the geology, history of the mining and ore processing activities, and environmental impact of the tailings on surrounding soils and ecosystems are given in other studies.<sup>4-9</sup> From 2021 the mine is owned by a Canadian company Trigon Metals. Production from the open pit recommenced in 2023 by mining the Cu ore with 1.2% average grade and re-opening activities of the underground mining are planned with ca. 726 kt of Cu ore grading around 2.7% mined annually in the coming years ([trigonmetals.com/kombat-mine](http://trigonmetals.com/kombat-mine)).<sup>3</sup>

The **Oamites** mine site is situated approximately 50 km south of Windhoek, the capital of Namibia, in the Khomas region in central Namibia. The mine was productive between 1971 and 1984. It extracted mostly Cu sulfide ores (Cu grade of 1.33 %) and produced approximately 5.5 Mt of tailings deposited in the two storage facilities.<sup>10-12</sup> Previous investigations demonstrated high metal(loid) concentrations in the tailings materials (e.g., up to 2697 mg/kg Cu)<sup>11</sup> and potential risk of their wind erosion and transport to various environmental compartments, including the large military base's inhabitants nearby.<sup>12,13,14</sup>

The **Namib Lead & Zinc** mine is located in the Rössing Mountain Area, in the Erongo region in western Namibia. This sulfidic Pb-Zn deposit was mined from 1968 to 1991 and the mining and ore processing activities were shortly renewed between 2019 and 2020 by the North River Resources company ([namibleadzinc.com](http://namibleadzinc.com); Daan Van Staden, 2023, personal communication). Today the mine is owned by Castlelake Group and is placed under care and maintenance. More details about the geology and the mineralization of the Namib Lead & Zinc mine is available in Basson et al.<sup>15</sup> Two mine tailings disposal sites are located southeast of the mine area. The older northern dump had a volume of ca. 4 Mm<sup>3</sup> of material, of which 1.25 Mm<sup>3</sup> was reworked for Zn in the mid-1990s, and residual tailings were placed in the southern dump.<sup>13,16,17</sup> The new tailings originating from the renewed mining and ore processing activities in 2019-2020 were also deposited in the southern dump (Daan Van Staden, 2023, personal communication).

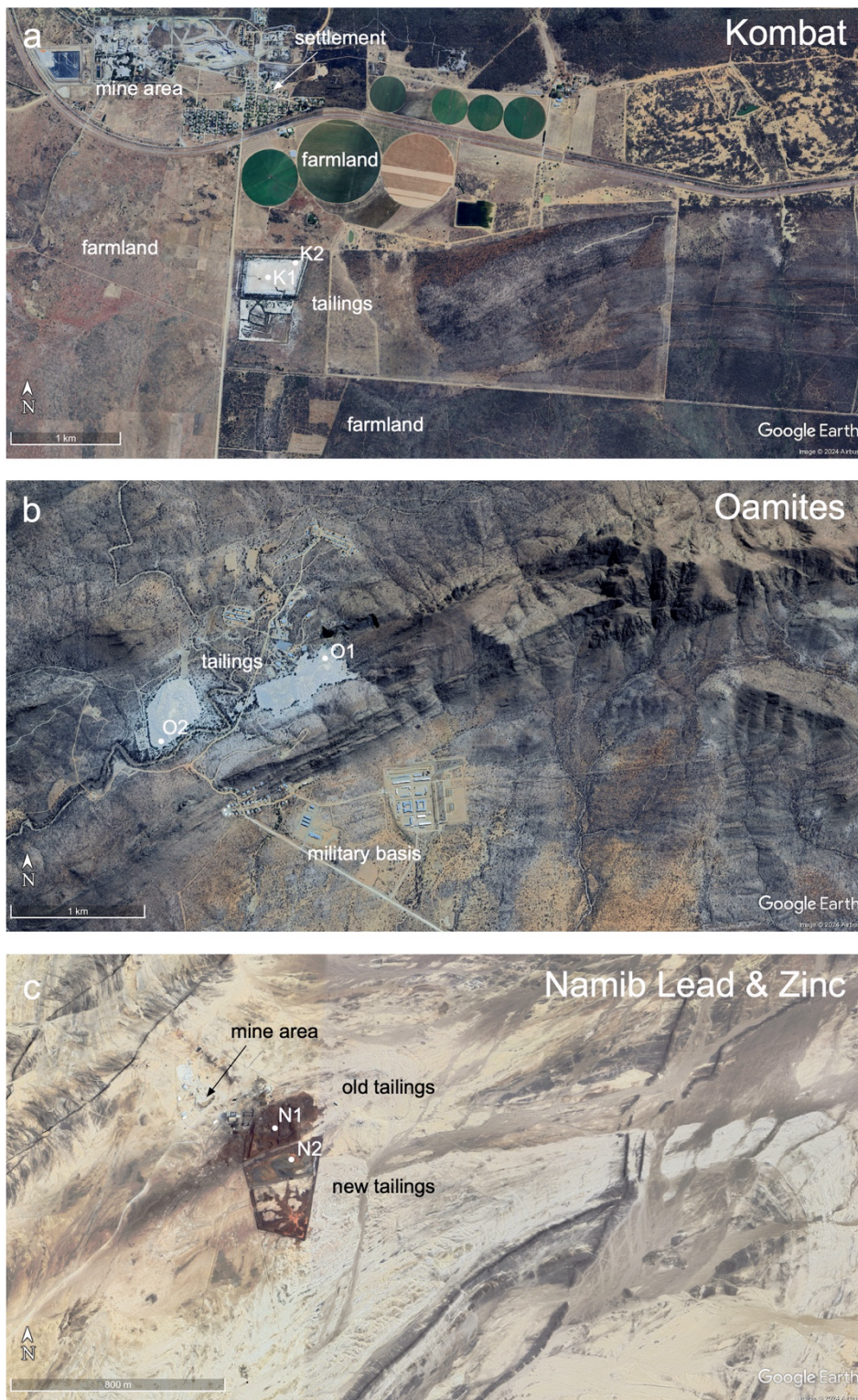


**Figure S2.** Satellite photographs (based on Google Earth™) of the study sites: Kombat (a), Oamites (b), and Namib Lead & Zinc (c) with indication of the tailings disposal sites, mine areas, settlements, and farmland.

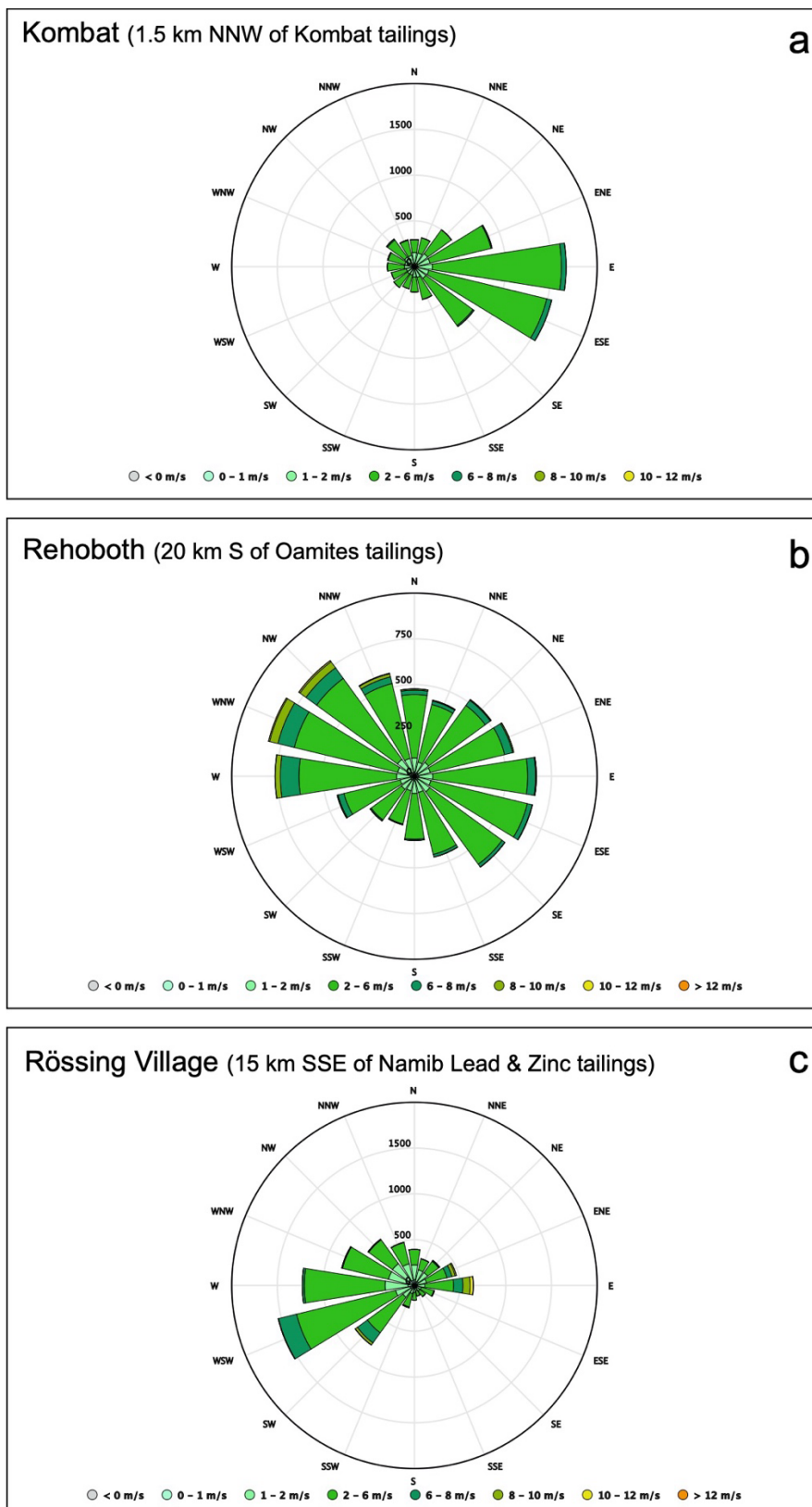


**Figure S3.** Wind roses and wind speed (in m/s) measured at meteorological stations located in the closest vicinity of the studied tailing disposal sites: Kombat (a), Oamites (b) and Namib Lead & Zinc (c) (adapted from MeteoBlue.com).

**Table S1.** Description and basic characteristics of the studied tailings.

Sample ID	Location	GPS coordinates	Sample type	Mineralization	Status
K1	Kombat	-19.72820, 17.71504	tailings 0-10 cm	Cu (+Pb, Zn, Ag)	closed, surface and underground mining planned (report 2024)
K2	Kombat	-19.72719, 17.71704	tailings 0-10 cm		
O1	Oamites	-22.97760, 17.07992	tailings 0-10 cm	Cu (+Ag)	closed
O2	Oamites	-22.98347, 17.06800	tailings 0-10 cm		
N1	Namib Lead & Zinc	-22.52004, 14.76123	old tailings 0-5 cm	Pb-Zn (+Ag)	care & maintenance
N2	Namib Lead & Zinc	-22.52113, 14.76188	new tailings (2019-2020) 0-5 cm		

Sample ID	Munsell color	pH	<48 µm fraction (%) <sup>*</sup>	<10 µm fraction (%) <sup>*</sup>
K1	5YR 7/2 (pinkish gray)	8.61 ± 0.00	82.0	0.5
K2	10R 6/4 (pale red)	8.28 ± 0.04	50.1	0.3
O1	2.5YR 7/1 (light gray)	8.63 ± 0.06	10.6	3.3
O2	2.5YR 7/2 (light gray)	8.65 ± 0.07	33.6	4.7
N1	10R 3/3 (dusky red)	5.98 ± 0.08	10.3	0.3
N2	2.5YR 3/6 (dark red)	6.30 ± 0.02	25.6	0.2

\* % of the original sample

**Table S2.** QC/QA results for the analysis of extracts and leachates (NIST 1643f and 1640a) and for the analysis of solids (NIST 2710a and 2711a).

(µg/L)		NIST 1643f (Trace elements in water)		(µg/L)		NIST 1640a (Trace elements in natural water)	
Element	n	Measured	Certified	Element	n	Measured	Certified
Ag	3	$0.97 \pm 0.02$	$0.9703 \pm 0.0055$	Ag	1	8	$8.081 \pm 0.046$
As	3	$54.15 \pm 0.63$	$57.42 \pm 0.38$	As		ND	$8.075 \pm 0.07$
Cd	3	$5.80 \pm 0.27$	$5.89 \pm 0.13$	Cd	1	4	$3.992 \pm 0.074$
Cr	3	$18.40 \pm 0.43$	$18.5 \pm 0.1$	Cr	1	42	$40.54 \pm 0.3$
Cu	3	$20.42 \pm 1.39$	$21.66 \pm 0.71$	Cu	2	$89.9 \pm 1.1$	$85.57 \pm 0.51$
Ni	3	$56.63 \pm 1.68$	$59.8 \pm 1.4$	Ni	1	26	$25.32 \pm 0.14$
Pb	3	$16.56 \pm 0.47$	$18.488 \pm 0.084$	Pb	1	14	$12.101 \pm 0.05$
Sb	3	$55.40 \pm 1.72$	$55.45 \pm 0.45$	Sb	1	7	$5.105 \pm 0.046$
V	3	$35.99 \pm 0.13$	$36.07 \pm 0.28$	V	1	15	$15.05 \pm 0.25$
Zn	3	$74.85 \pm 0.93$	$74.4 \pm 1.7$	Zn	2	$58 \pm 0.0$	$55.64 \pm 0.35$
(mg/kg)		NIST 2710a (Montana I soil)		(mg/kg)		NIST 2711a (Montana II soil)	
Element	n	Measured	Certified	Element	n	Measured	Certified
Ag	3	$40 \pm 1$	<u>40</u>	Ag	3	$6.1 \pm 0.2$	<u>6</u>
As	3	$1,394 \pm 6$	$1,540 \pm 10$	As	3	$95 \pm 1$	$107 \pm 5$
Cd	3	$11.2 \pm 0.6$	$12.3 \pm 0.3$	Cd	3	$49.0 \pm 3.0$	$54.1 \pm 0.5$
Cr	3	$28 \pm 7$	$23 \pm 6$	Cr	5	$93 \pm 26$	$52.3 \pm 2.9$
Cu	5	$3,105 \pm 278$	$3,420 \pm 50$	Cu	5	$126 \pm 7$	$140 \pm 2$
Ni	2	$24 \pm 17$	$8 \pm 1$	Ni	2	$29.7 \pm 10.6$	$21.7 \pm 0.7$
Pb	5	$5,230 \pm 212$	$5,520 \pm 30$	Pb	5	$1,278 \pm 52$	$1,400 \pm 10$
Sb	3	$50 \pm 2$	$52.5 \pm 1.6$	Sb	3	$23.1 \pm 1.4$	$23.8 \pm 1.4$
V	5	$78 \pm 6$	$82 \pm 9$	V	5	$77.6 \pm 4.3$	$80.7 \pm 5.7$
Zn	5	$4,134 \pm 162$	$4,180 \pm 20$	Zn	5	$400 \pm 4$	$414 \pm 11$

ND = not determined

*Italics* = reference values Underlined = information values

**Table S3.** Conditions and standards used for the EPMA measurements.

<b>Silicates and oxides (accelerating voltage: 15 kV, beam current: 10 nA)</b>				
Element	X-ray	Crystal	Standard	DL (wt% oxide)
Si	Ka	TAP	Diopside	0.052
Al	Ka	TAP	Pyrope	0.037
K	Ka	PETJ	Sanidine	0.023
Ca	Ka	PETJ	Diopside	0.033
S	Ka	PETJ	Anhydrite	0.101
Cl	Ka	PETJ	Tugtupite	0.016
Ba	La	PETJ	Barite	0.073
Ti	Ka	PETJ	Rutile	0.062
Pb	Ma	PETJ	Crocoite	0.072
Cr	Ka	PETJ	Chromium oxide	0.062
Fe	Ka	LIFL	Magnetite	0.043
Mn	Ka	LIFL	Rhodonite	0.043
Zn	Ka	LIFL	Willemite	0.087
Cu	Ka	LIFL	Cuprite	0.055
Ni	Ka	LIFL	Pentlandite	0.048
Na	Ka	TAP	Albite	0.038
Mg	Ka	TAP	MgO	0.023
As	La	TAP	Skutterudite	0.046
<b>Sulfides (accelerating voltage: 15 kV, beam current: 20 nA)</b>				
Element	X-ray	Crystal	Standard	DL (wt% element)
As	La	TAP	Skutterudite	0.013
Pb	Ma	PETJ	Galena	0.033
S	Ka	PETJ	Sphalerite	0.009
Cu	Ka	LIF	Cuprite	0.025
Zn	Ka	LIF	Willemite	0.036
Fe	Ka	LIFL	Magnetite	0.014

**Table S4.** QC/QA results for the bioaccessible concentrations of Pb and As in standard reference materials (SRM) NIST 2710a and 2711a according to US EPA Method 1340 bioaccessibility extraction test.<sup>18</sup>

<b>NIST 2710a (Montana I soil)</b>						
Element	<i>n</i>	Measured (mg/kg)	Measured BAF (%)	Reported BAF (%)*	Certified BAF (%)	
					Mean	Range
Pb	4	3,377 ± 160	61.2 ± 2.9	56.1 ± 4.6	67.5	60.7–74.2
As	4	549 ± 16	35.6 ± 1.0	27.4 ± 5.7		
<b>NIST 2711a (Montana II soil)</b>						
Element	<i>n</i>	Measured (mg/kg)	Measured BAF (%)	Reported BAF (%)*	Certified BAF (%)	
					Mean	Range
Pb	4	1,234 ± 75	88.2 ± 5.3	88.8 ± 5.7	88.7	75.2–96.2
As	3	57.1 ± 0.2	53.3 ± 0.2	56.1 ± 4.6		

\* Reported in Dodd et al. (2024)<sup>19</sup>

**Table S5.** Phase compositions of the original tailings based on X-ray diffraction analysis.

Code	Calcite CaCO <sub>3</sub>	Dolomite CaMg(CO <sub>3</sub> ) <sub>2</sub>	Mica see footnote <sup>a</sup>	Quartz SiO <sub>2</sub>	Feldspar see footnote <sup>b</sup>	Goethite FeOOH	Lepidocrocite FeOOH	Hematite Fe <sub>2</sub> O <sub>3</sub>	Malachite Cu <sub>2</sub> (CO <sub>3</sub> )(OH) <sub>2</sub>
K1	***	***	**	*		tr			tr
K2	***	***	**	**				tr	
O1			***	***	***				
O2			**	**	***				
N1	*		*	**		*	tr		
N2	*		*	*			tr		

Code	Gypsum CaSO <sub>4</sub> ·2H <sub>2</sub> O	Hexahydrite MgSO <sub>4</sub> ·6H <sub>2</sub> O	Titanite CaTiSiO <sub>5</sub>	Siderite FeCO <sub>3</sub>	Sphalerite ZnS	Pyrrhotite Fe <sub>1-x</sub> S	Pyrite FeS <sub>2</sub>	Halite NaCl	Sulfur S
K1									
K2	tr	*							
O1			tr						
O2			tr						
N1	***			tr	tr			tr	
N2	***				tr		*		*

Relative abundances of phases were estimated from XRD patterns using the relative intensity ratio (RIR) method: \*\*\* abundant, \*\* common, \* minor, tr trace.

<sup>a</sup> Mica = muscovite [KAl<sub>2</sub>(Si<sub>3</sub>Al)O<sub>10</sub>(OH,F)<sub>2</sub>] and/or biotite [K(Mg,Fe)<sub>3</sub>(AlSi<sub>3</sub>)O<sub>10</sub>(OH,F)<sub>2</sub>]

<sup>b</sup> Feldspar = albite (NaAlSi<sub>3</sub>O<sub>8</sub>) and/or orthoclase (KAlSi<sub>3</sub>O<sub>8</sub>)

**Table S6.** Selected microprobe analyses of sulfides (in wt% and at%) and calculated empirical formulae (apfu – atoms per formula unit).

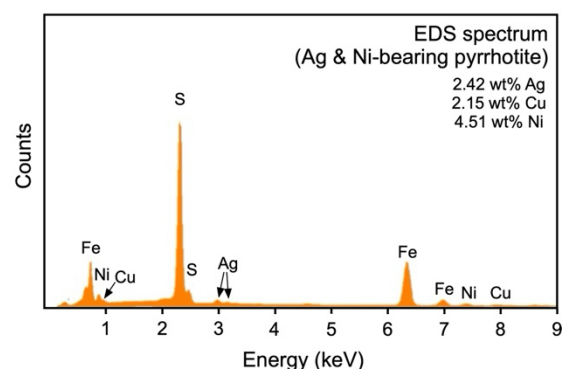
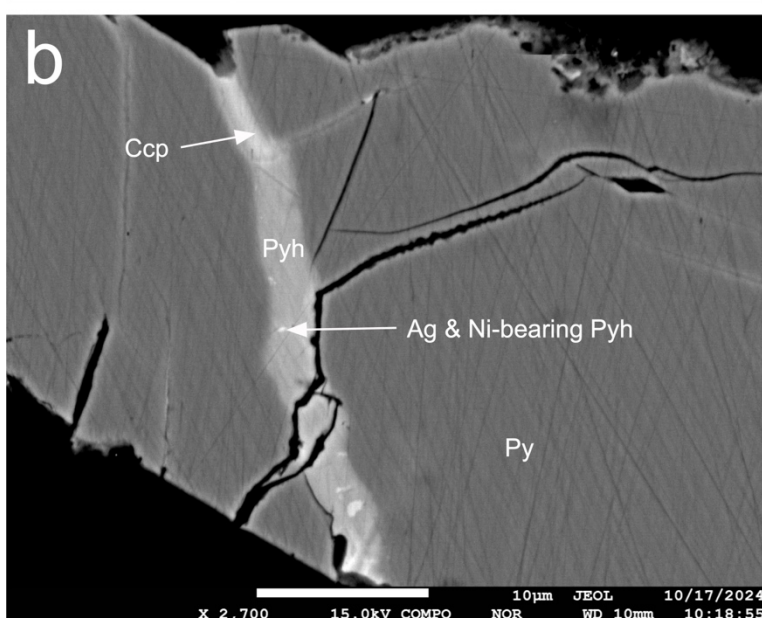
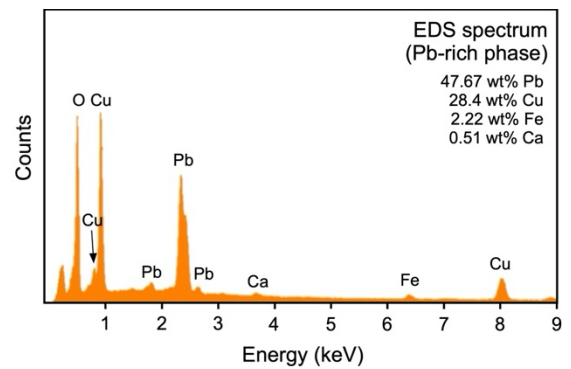
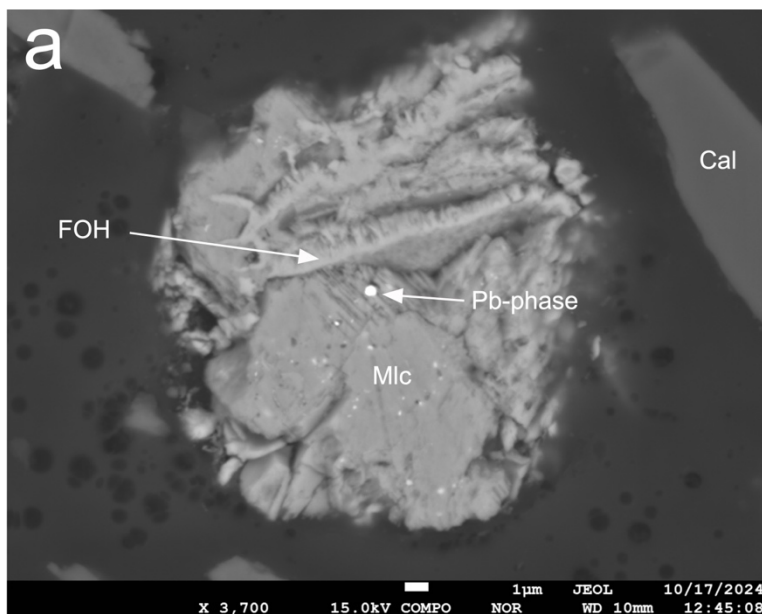
Sample	N1	O1	N2	O1	O1	N2	N2
Spot no.	4	11	8	12	14	6	7
Phase	pyrrhotite	pyrrhotite	pyrite	pyrite	chalcopyrite	Fe sphalerite	sphalerite
wt%							
Fe	59.09	58.13	47.29	44.83	28.91	11.19	1.86
Cu	–	1.08	–	0.04	32.11	0.06	–
Zn	0.07	0.07	0.07	–	–	54.52	63.62
Pb	–	0.17	0.16	–	0.11	0.05	0.19
As	–	–	–	–	–	–	–
S	38.96	37.07	53.36	53.49	33.71	33.43	32.10
Total	98.13	96.53	100.88	98.37	94.85	99.25	97.77
at%							
Fe	46.52	46.97	33.70	32.47	24.95	9.64	1.65
Cu	0.00	0.77	0.00	0.03	24.36	0.05	0.00
Zn	0.05	0.05	0.04	0.00	0.00	40.13	48.45
Pb	0.00	0.04	0.03	0.00	0.03	0.01	0.05
As	0.00	0.00	0.00	0.00	0.00	0.00	0.00
S	53.43	52.18	66.23	67.50	50.67	50.17	49.85
apfu							
Fe	0.87	0.90	1.02	0.96	0.49	0.19	0.03
Cu	0.00	0.01	0.00	0.00	0.48	0.00	0.00
Zn	0.00	0.00	0.00	0.00	0.00	0.80	0.97
Pb	0.00	0.00	0.00	0.00	0.00	0.00	0.00
As	0.00	0.00	0.00	0.00	0.00	0.00	0.00
S	1.00	1.00	2.00	2.00	1.00	1.00	1.00

**Table S7.** Selected microprobe analyses of various Fe (oxyhydr)oxides (FOH), Fe sulfates, and carbonates (in wt%).

Sample	O1	K1	K1	N1	N1	K1	N2	N2	K1
Spot	1	5	18	24	25	13	19	22	4
Phase	FOH	FOH	FOH	FOH	FOH	hematite	jarosite	jarosite	mixture
SiO <sub>2</sub>	5.29	0.92	7.23	0.30	0.39	—	0.24	0.18	8.29
TiO <sub>2</sub>	—	—	—	—	—	—	—	—	—
Al <sub>2</sub> O <sub>3</sub>	0.14	0.22	0.31	0.06	—	—	—	0.14	1.93
Cr <sub>2</sub> O <sub>3</sub>	—	—	—	—	—	—	—	—	—
Fe <sub>2</sub> O <sub>3</sub>	49.09	81.91	63.00	79.67	82.16	97.06	36.70	51.25	16.79
MnO	0.36	—	0.68	0.11	1.17	—	—	0.14	6.62
MgO	0.13	—	0.34	0.06	0.12	—	0.08	0.05	0.20
CaO	1.19	0.68	1.72	0.13	0.22	1.01	0.24	0.16	2.72
Na <sub>2</sub> O	—	—	0.11	—	—	0.24	0.48	0.16	—
K <sub>2</sub> O	—	—	—	—	0.03	—	0.15	0.10	—
BaO	—	—	0.09	—	—	—	—	—	—
CuO	17.07	0.38	1.54	—	—	0.07	0.12	—	5.17
PbO	7.18	0.40	11.78	—	0.64	0.11	1.22	0.20	31.67
ZnO	1.18	—	2.51	0.16	0.38	0.09	0.15	0.26	0.11
NiO	—	—	—	—	0.05	—	—	—	—
As <sub>2</sub> O <sub>5</sub>	—	0.07	—	0.06	—	—	—	—	0.74
SO <sub>3</sub>	1.36	0.14	—	1.68	5.24	0.12	15.60	13.20	
Cl	—	—	0.07	0.08	0.03	0.02	0.82	0.19	0.17
Total	78.08	76.52	83.06	74.32	82.18	98.71	55.80	66.01	74.40

Sample	K1	K1	K1	K1	K1
Spot	15	16	17	9	11
Phase	dolomite	calcite	siderite	malachite	malachite
SiO <sub>2</sub>	—	—	—	0.12	—
TiO <sub>2</sub>	—	—	—	0.19	0.13
Al <sub>2</sub> O <sub>3</sub>	—	—	0.05	0.09	0.04
Cr <sub>2</sub> O <sub>3</sub>	—	—	—	—	—
FeO	0.07	—	38.28	0.52	0.38
MnO	—	0.29	4.39	—	0.06
MgO	20.99	0.19	3.37	—	0.05
CaO	31.32	56.61	3.98	0.47	0.98
Na <sub>2</sub> O	—	—	0.18	—	—
K <sub>2</sub> O	—	—	—	0.04	—
BaO	—	—	—	0.32	0.32
CuO	0.06	—	—	63.32	66.30
PbO	—	0.14	—	0.24	0.09
ZnO	—	—	6.77	—	—
NiO	—	—	—	—	—
As <sub>2</sub> O <sub>5</sub>	—	—	—	—	—
SO <sub>3</sub>	—	—	—	—	1.25
Cl	0.03	0.02	—	0.02	—
CO <sub>2</sub> (calc)	47.66	44.93	36.71	17.96	18.98
H <sub>2</sub> O	—	—	—	—	—
Total	100.11	102.18	93.73	83.28	88.58



**Figure S4.** Scanning electron micrographs in back-scattered electrons (BSE) of trace metal-bearing particles. (a) Pb-bearing phase (probably cerussite,  $\text{PbCO}_3$ ) forming submicron inclusions in a grain composed of malachite and Fe (oxyhydr)oxides (tailings K1); (b) Ag- and Ni-bearing pyrrhotite inclusions in a vein composed in metal-free pyrrhotite and chalcopyrite embedded within a pyrite grain (tailings O1). Abbreviations according to Warr (2021)<sup>20</sup>: Cal – calcite, Ccp – chalcopyrite, FOH – Fe (oxyhydr)oxide, Mlc – malachite, Py – pyrite, Pyh – pyrrhotite.

**Table S8.** Total and bioaccessible concentrations of contaminants in the original tailings and the <48 µm and <10 µm dust fractions (mg/kg) (mean values ± standard deviation, n = 2).

Totals	Ag	As	Cd	Cr	Cu	Ni	Pb	Sb	V	Zn
K1 original	1.83	63.2	10.9	16.0	9,380	77.1	3,700	3.48	63.1	131
K1 <48 µm	2.88	66.7	9.06	8.43	10,500	3.42	3,460	3.25	59.6	125
K1 <10 µm	7.51	134	11.8	36.4	14,900	14.3	8,880	6.41	105	229
K2 original	1.04	25.6	2.66	17.6	1,480	3.50	977	10.3	148	106
K2 <48 µm	1.13	19.9	2.07	28.6	1,130	8.15	803	6.29	165	84.8
K2 <10 µm	2.01	35.7	3.45	52.8	2,120	16.9	1,620	12.3	197	167
O1 original	5.40	2.03	0.61	20.1	1,320	11.6	269	0.61	153	115
O1 <48 µm	6.03	3.44	1.33	101	1,510	49.5	424	0.82	355	234
O1 <10 µm	22.7	8.53	4.06	166	4,220	92.4	1,350	1.53	220	622
O2 original	2.49	5.29	0.21	82.7	1,700	18.0	115	0.68	192	60.0
O2 <48 µm	3.65	9.22	0.35	153	2,790	26.6	205	0.69	220	70.0
O2 <10 µm	12.7	26.0	0.94	704	5,790	41.4	629	2.02	152	120
N1 original	13.7	128	46.0	8.53	158	4.14	6,930	16.5	14.3	12,600
N1 <48 µm	11.3	102	34.2	22.5	290	13.3	3,520	12.0	17.8	12,000
N1 <10 µm	12.5	89.9	16.1	16.6	361	8.70	4,690	9.77	10.9	8,250
N2 original	7.56	69.2	48.6	29.4	172	7.96	1,310	6.56	16.4	13,300
N2 <48 µm	6.69	86.0	22.7	60.2	180	25.7	2,110	4.85	14.0	7,760
N2 <10 µm	4.63	63.3	15.9	79.1	250	11.9	3,480	8.34	17.1	6,320
Min	1.04	2.03	0.21	8.43	158	3.42	115	0.61	10.9	60.0
Max	22.70	134	48.6	704	14,900	92.4	8,880	16.5	355	13,300
Mean	6.99	52.1	12.8	89.1	3,236	24.1	2,471	5.91	118	3,461
Median	5.72	49.5	6.56	32.9	1,495	13.8	1,485	5.57	127	198
Bioaccessible										
K1 original	2.98 ± 0.43	49.4 ± 2.72	10.1 ± 0.14	<1.9	7,710 ± 258	3.64 ± 0.14	3,040 ± 211	1.76 ± 0.18	25.0 ± 1.90	123 ± 9
K1 <48 µm	2.28 ± 0.04	51.9 ± 0.40	9.89 ± 0.02	<1.9	8,810 ± 56	3.87 ± 0.17	3,250 ± 3	1.73 ± 0.08	24.1 ± 1.62	175 ± 29
K1 <10 µm	6.10	105	11.8	2.58	12,000	4.84	70,70	4.42	53.9	203
K2 original	0.96 ± 0.07	12.9 ± 1.13	2.19 ± 0.06	<1.9	1,100 ± 8	2.73 ± 0.04	719 ± 29	2.62 ± 0.18	<0.5	71.9 ± 0.03
K2 <48 µm	0.87 ± 0.02	11.2 ± 0.63	2.11 ± 0.14	<1.9	866 ± 12	3.13 ± 0.05	647 ± 17	2.58 ± 0.44	<0.5	63.9 ± 4.6
K2 <10 µm	1.89	17.5	3.17	2.73	1,510	4.51	1,150	4.24	3.13	93.8
O1 original	2.17 ± 0.002	<1	0.42 ± 0.03	<1.9	627 ± 58	1.63 ± 0.12	141 ± 8	0.15 ± 0.00	2.69 ± 0.29	84.2 ± 8.4
O1 <48 µm	4.65 ± 0.89	1.12 ± 0.00	0.95 ± 0.05	2.74 ± 0.02	1,130 ± 6	4.45 ± 0.03	294 ± 5	0.54 ± 0.19	4.66 ± 0.13	230 ± 46
O1 <10 µm	21.9	3.20	4.16	13.2	4,110	19.3	1,220	0.99	12.12	596
O2 original	1.37 ± 0.04	1.55 ± 0.09	<0.1	4.12 ± 0.06	1,120 ± 63	2.22 ± 0.08	60.2 ± 1.7	0.60 ± 0.00	5.79 ± 0.35	48.6 ± 18
O2 <48 µm	2.33 ± 0.12	2.96 ± 0.26	0.19 ± 0.04	9.65 ± 0.40	2,020 ± 60	13.4 ± 8.80	109 ± 3	0.42 ± 0.00	6.83 ± 0.23	20.2 ± 0.1
O2 <10 µm	11.6	8.86	0.77	36.0	5,450	15.4	418	0.07	13.37	112
N1 original	1.68 ± 0.09	<1	3.16 ± 0.19	<1.9	20.6 ± 5.0	2.14 ± 0.85	440 ± 47	0.19 ± 0.04	<0.5	689 ± 0.2
N1 <48 µm	2.68 ± 0.34	<1	3.48 ± 0.02	<1.9	25.1 ± 1.8	1.22 ± 0.18	794 ± 27	0.27 ± 0.10	<0.5	882 ± 6

N1 <10 $\mu\text{m}$	2.82	<1	5.15	<1.9	48.2	1.73	1,430	0.49	<0.5	1,480
N2 original	1.06 $\pm$ 0.03	<1	2.89 $\pm$ 0.23	<1.9	90.2 $\pm$ 5.2	1.13 $\pm$ 0.13	366 $\pm$ 24	<0.02	<0.5	391 $\pm$ 9
N2 <48 $\mu\text{m}$	0.85 $\pm$ 0.03	<1	4.05 $\pm$ 0.22	<1.9	86.0 $\pm$ 0.1	1.11 $\pm$ 0.09	557 $\pm$ 3	<0.02	<0.5	607 $\pm$ 4
N2 <10 $\mu\text{m}$	0.99	<1	6.73	<1.9	156	1.79	1,040	<0.02	<0.5	1,210
Min	0.85	<1	<0.1	<1.9	20.6	1.11	60.2	<0.02	<0.5	20.2
Max	21.9	105	11.8	36.0	12,000	19.3	7,070	4.42	53.9	1,480
Mean	3.84	24.1	4.19	10.1	2,604	4.90	1,264	1.40	15.2	393
Median	2.23	11.2	3.17	4.12	1,110	2.93	683	0.60	9.48	189

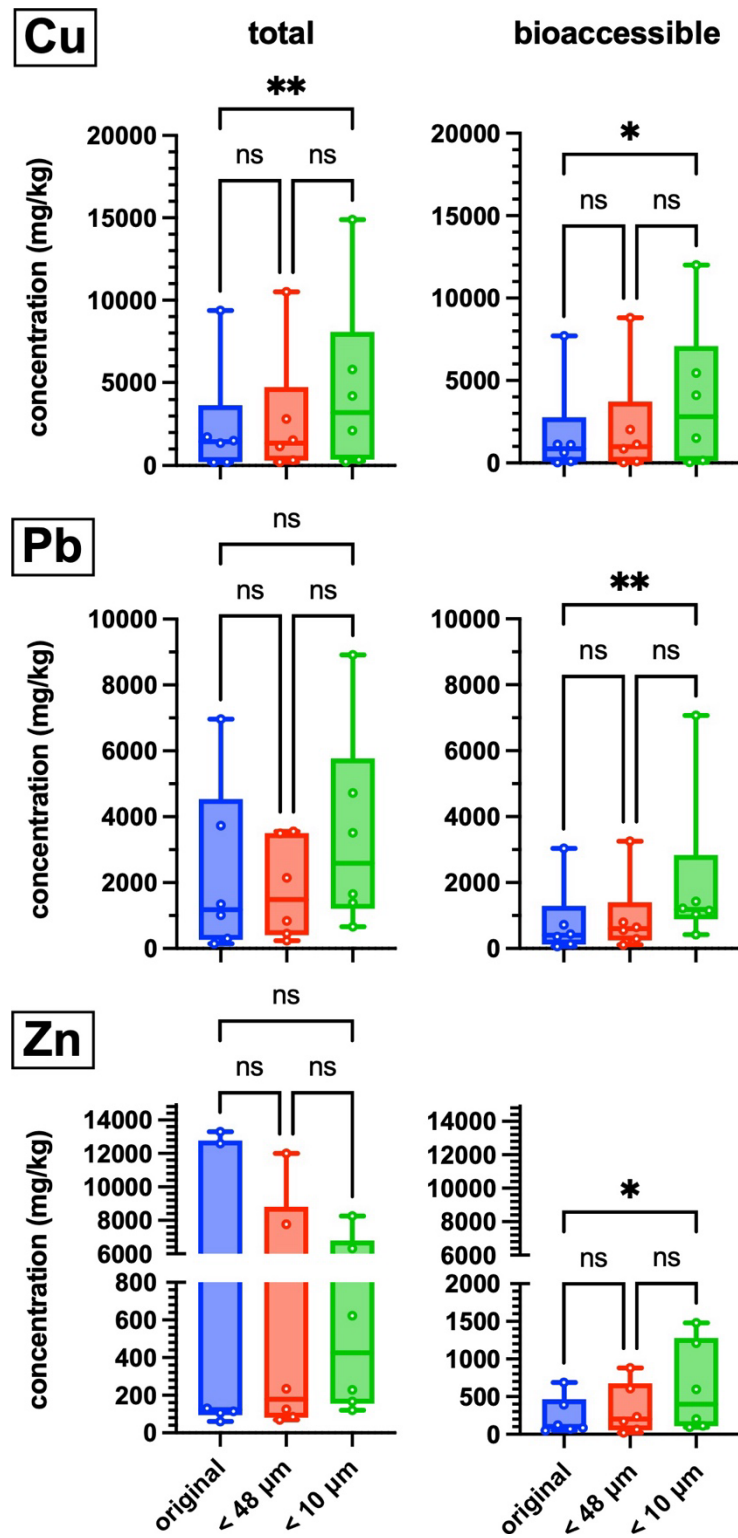


**Figure S5.** Comparisons of total and bioaccessible Cu, Pb, and Zn concentrations in original tailings and <48 μm and <10 μm dust fractions for the entire dataset (data points correspond to mean values for duplicated analyses). Calculations using the Dunn's multiple comparison test (alpha = 0.05) indicate whether the differences are statistically significant (indicated by \*) or not (ns).

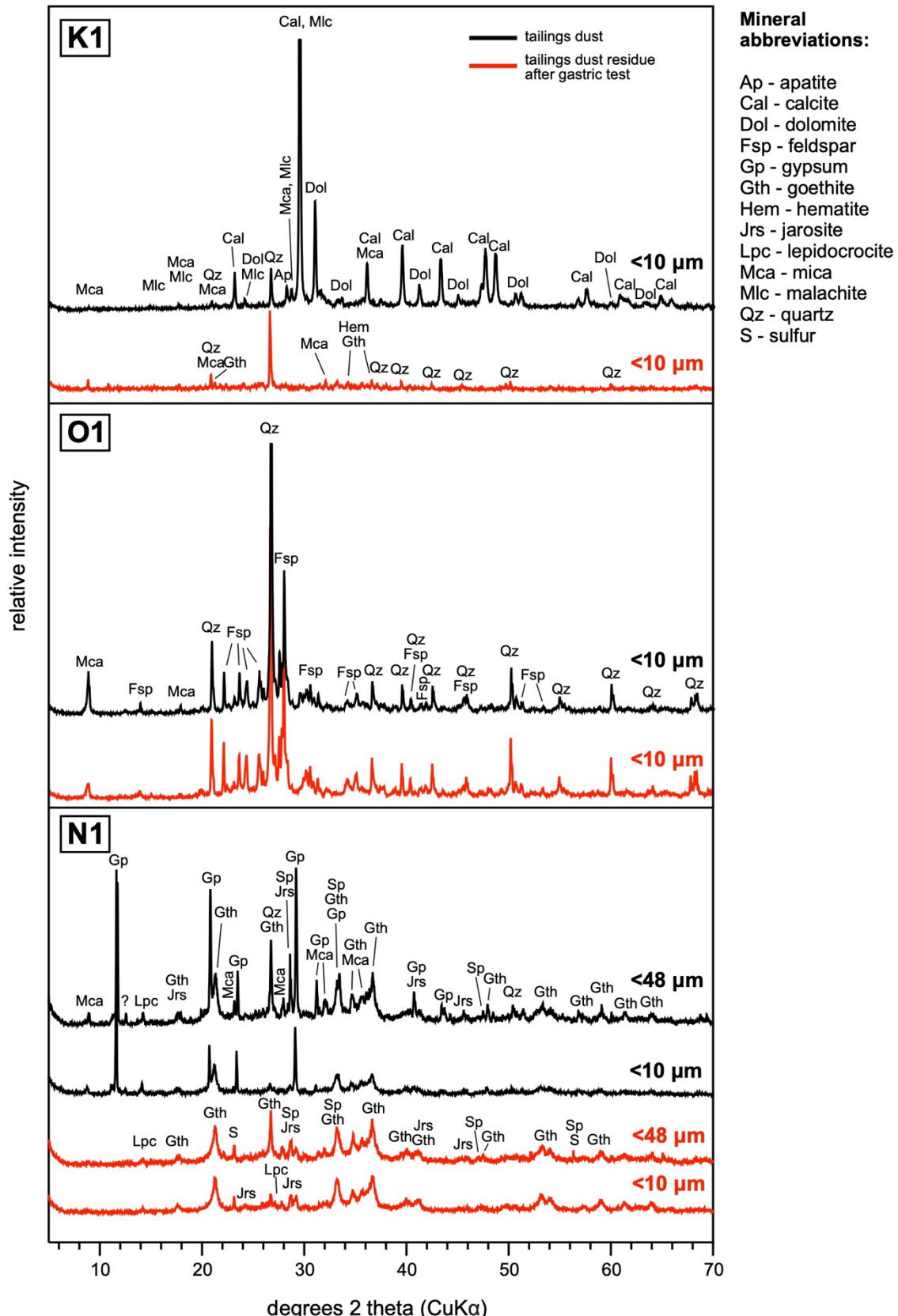


**Figure S6.** X-ray powder diffraction patterns of selected tailings dust fractions and residues after the leaching test using simulated gastric fluid (SGF) (only 5-70° 2-theta range is shown).

**Table S9.** Exposure estimates calculated as daily intakes of individual contaminants (in µg/d) assuming the dust intake of 100 mg/d and 280 mg/d (mean values) and comparisons with background exposure (BE), tolerable daily intake (TDI) limits, Agency for Toxic Substances and Disease Registry (ATSDR) minimal risk levels and US Environmental Protection Agency (US EPA) reference dose (RfD) values calculated for a 10-kg child and a 70-kg adult. Different colors and fonts are used for better orientation.

Code	Ag	As	Cd	Cu	Cr(VI)	Ni	Pb	Sb	V	Zn
<b>Limit (µg/kg<sub>bw</sub>/d)</b>										
BE <sup>a</sup>	0.3	0.22/0.17 <sup>d</sup>		30	4.30E-04 <sup>e</sup>	4	0.6/2.0 <sup>f</sup>	0.4	0.3	300
<b>TDI<sup>a</sup></b>	<b>1</b>	<b>0.5</b>		<b>140</b>	<b>5</b>	<b>50</b>	<b>3.6</b>	<b>6</b>	<b>2</b>	<b>500</b>
<b>TDI (EFSA)<sup>b</sup></b>		<b>0.36</b>				<b>2.8</b>				
ATSDR acute <sup>c</sup>	5			20				1000		
ATSDR chronic <sup>c</sup>	0.3	0.1			0.9					300
ATSDR intermediate <sup>c</sup>		0.5		20	5		0.6	10	300	
US EPA RfD 2024	5	0.3	0.1	40	3	11	0.4	5.04	300	
<b>10-kg child (µg/d)</b>										
<b>TDI</b>	<b>10</b>	<b>5</b>		<b>1,400</b>	<b>50</b>	<b>500</b>	<b>36</b>	<b>60</b>	<b>20</b>	<b>5,000</b>
<b>TDI (EFSA)</b>		<b>3.6</b>				<b>28</b>				
ATSDR acute	50			200				10,000		
ATSDR chronic	3	1			9					3,000
ATSDR intermediate		5		200	50		6	100	3,000	
US EPA RfD 2024	50	3	1	400	30	110	4	50.4	3,000	
<b>70-kg adult (µg/d)</b>										
<b>TDI</b>	<b>70</b>	<b>35</b>		<b>9,800</b>	<b>350</b>		<b>252</b>	<b>420</b>	<b>140</b>	<b>35,000</b>
<b>TDI (EFSA)</b>		<b>25.2</b>				<b>196</b>				
ATSDR acute	350			1,400				70,000		
ATSDR chronic	21	7			63					21,000
ATSDR intermediate		35		1,400	350		42	700	21,000	
US EPA RfD 2024	350	21	7	2,800	210	770	28	352.8	21,000	
<b>Exposure: 100 mg/d</b>										
K1 original	0.30	<b>4.94</b>	<b>1.01</b>	<b>770</b>	<0.19	0.36	<b>304</b>	0.18	2.50	12.3
K1 <48 µm	0.23	<b>5.19</b>	0.99	<b>881</b>	<0.19	0.39	<b>325</b>	0.17	2.41	17.5
K1 <10 µm	0.61	<b>10.5</b>	<b>1.18</b>	<b>1,197</b>	0.26	0.48	<b>707</b>	0.44	5.39	20.3
K2 original	0.10	1.29	0.22	110	<0.19	0.27	<b>71.9</b>	0.26	<0.05	7.19
K2 <48 µm	0.09	1.12	0.21	87	<0.19	0.31	<b>64.7</b>	0.26	<0.05	6.39
K2 <10 µm	0.19	1.75	0.32	151	0.27	0.45	<b>115</b>	0.42	0.31	9.38
O1 original	0.22	<0.1	0.04	63	<0.19	0.16	14.1	0.01	0.27	8.42
O1 <48 µm	0.47	0.11	0.10	112	0.27	0.44	29.4	0.05	0.47	23.0
O1 <10 µm	2.19	0.32	0.42	<b>411</b>	1.32	1.93	<b>122</b>	0.10	1.21	59.6
O2 original	0.14	0.16	<0.01	112	0.41	0.22	6.02	0.06	0.58	4.86
O2 <48 µm	0.23	0.30	0.02	<b>202</b>	0.96	1.34	10.9	0.04	0.68	2.02
O2 <10 µm	1.16	0.89	0.08	<b>545</b>	3.60	1.54	<b>41.8</b>	0.01	1.34	11.2
N1 original	0.17	<0.1	0.32	2.06	<0.19	0.21	<b>44.0</b>	0.02	<0.05	68.9
N1 <48 µm	0.27	<0.1	0.35	2.51	<0.19	0.12	<b>79.4</b>	0.03	<0.05	88.2
N1 <10 µm	0.28	<0.1	0.51	4.82	<0.19	0.17	<b>143</b>	0.05	<0.05	148
N2 original	0.11	<0.1	0.29	9.02	<0.19	0.11	<b>36.6</b>	<0.02	<0.05	39.1
N2 <48 µm	0.08	<0.1	0.41	8.60	<0.19	0.11	<b>55.7</b>	<0.02	<0.05	60.7
N2 <10 µm	0.10	<0.1	0.67	15.6	<0.19	0.18	<b>104</b>	<0.02	<0.05	120
<b>Exposure: 280 mg/d</b>										
K1 original	0.83	<b>13.8</b>	<b>2.81</b>	<b>2,157</b>	<0.53	1.02	<b>851</b>	0.49	7.00	34.5
K1 <48 µm	0.64	<b>14.5</b>	<b>2.77</b>	<b>2,467</b>	<0.53	1.08	<b>911</b>	0.48	6.74	48.9
K1 <10 µm	1.71	<b>29.4</b>	<b>3.32</b>	<b>3,351</b>	0.72	1.35	<b>1,979</b>	1.24	15.1	56.8
K2 original	0.27	<b>3.61</b>	0.61	<b>308</b>	<0.53	0.76	<b>201</b>	0.73	<0.14	20.1
K2 <48 µm	0.24	<b>3.14</b>	0.59	<b>243</b>	<0.53	0.88	<b>181</b>	0.72	<0.14	17.9
K2 <10 µm	0.53	<b>4.89</b>	0.89	<b>423</b>	0.76	1.26	<b>323</b>	1.19	0.88	26.3
O1 original	0.61	<0.28	0.12	176	<0.53	0.46	<b>39.4</b>	0.04	0.75	23.6
O1 <48 µm	1.30	0.31	0.27	<b>315</b>	0.77	1.25	<b>82.4</b>	0.15	1.31	64.5
O1 <10 µm	6.13	0.90	<b>1.17</b>	<b>1151</b>	3.69	5.41	<b>342</b>	0.28	3.39	167

O2 original	0.38	0.43	<0.028	<b>314</b>	1.15	0.62	16.9	0.17	1.62	13.6
O2 <48 µm	0.65	0.83	0.05	<b>566</b>	2.70	3.75	30.6	0.12	1.91	5.65
O2 <10 µm	3.25	2.48	0.22	<b>1,526</b>	<b>10.1</b>	4.31	<b>117</b>	0.02	3.74	31.4
N1 original	0.47	<0.28	0.89	5.78	<0.53	0.60	<b>123</b>	0.05	<0.14	193
N1 <48 µm	0.75	<0.28	0.97	7.03	<0.53	0.34	<b>222</b>	0.07	<0.14	247
N1 <10 µm	0.79	<0.28	<b>1.44</b>	13.5	<0.53	0.48	<b>401</b>	0.14	<0.14	415
N2 original	0.30	<0.28	0.81	25.3	<0.53	0.32	<b>102</b>	<0.06	<0.14	109
N2 <48 µm	0.24	<0.28	<b>1.14</b>	24.1	<0.53	0.31	<b>156</b>	<0.06	<0.14	170
N2 <10 µm	0.28	<0.28	<b>1.88</b>	43.8	<0.53	0.50	<b>291</b>	<0.06	<0.14	337

<sup>a</sup> defined in Baars et al. (2001)<sup>21</sup> and Tiesjema and Baars (2009)<sup>22</sup>

<sup>b</sup> defined by the European Food Safety Authority (EFSA)

<sup>c</sup> defined by Agency for Toxic Substances and Disease Registry (ATSDR)<sup>23</sup> as Minimal Risk following durations: acute = 1 to 14 days, intermediate = 15 to 364 days, chronic = 1 year or longer

<sup>d</sup> 0.22 for men, 0.17 for women

<sup>e</sup> maximum background exposure

<sup>f</sup> 0.6 for adult, 2 for children

Exposure exceedance of the minimal reference values for children is indicated in **bold** and for both adults and children by **bold italics**.

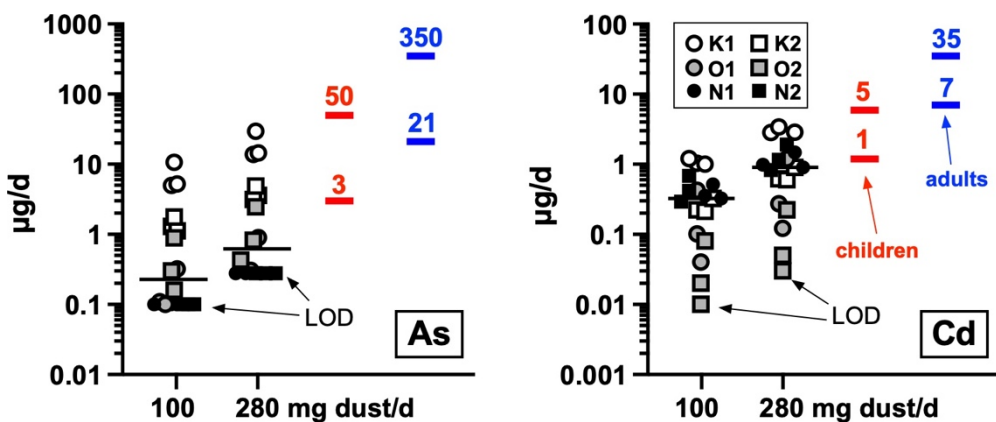


**Figure S7.** Exposure estimates calculated as daily intakes of minor contaminants, As and Cd (in  $\mu\text{g}/\text{d}$ ), assuming a dust intake of 100  $\text{mg}/\text{d}$  and 280  $\text{mg}/\text{d}$  and a comparison with ATSDR minimal risk levels calculated for a 10-kg child and a 70-kg adult, respectively (other contaminants). Upper limit values correspond to “acute” (As) or “intermediate” (Cd) exposure, and the lower limit values correspond to “chronic” exposure. Black lines indicate the median value for the entire dataset; K = Kombat, O = Oamites, N = Namib Lead & Zinc.

## References:

- (1) M. New, M. Hulme and P. Jones, Representing twentieth-century space-time climate variability. Part I: Development of a 1961–90 mean monthly terrestrial climatology, *J. Climate*, 1999, **12**, 829–856. [https://doi.org/10.1175/1520-0442\(1999\)012<0829:RTCSTC>2.0.CO;2](https://doi.org/10.1175/1520-0442(1999)012<0829:RTCSTC>2.0.CO;2)
- (2) F1 project, *GIS-based Atlas of Holocene Land Use Potential for Selected Research Areas*. (<https://www.uni-koeln.de/sfb389/e/e1/index.htm>)
- (3) J. Mainama, M. Wanless, J. van Graan and A. McDonald, *Independent Technical Report for Kombat’s Asis West Mine, Namibia (Technical Report No. 604971)*, SRK Consulting, Johannesburg, South Africa, 2024.
- (4) J.G. Deane, The structural evolution of the Kombat deposits, Otavi Mountainland, Namibia, *Comm. Geol. Survey Namibia*, 1995, **10**, 99–107.
- (5) I. Mapaure, P.M. Chimwamurombe, B.S. Mapani and F. Kamona, Impacts of mine dump pollution on plant species diversity, composition and structure of semiarid savanna in Namibia, *Afr. J. Range For. Sci.*, 2011, **28**, 149–154. <https://doi.org/10.2989/10220119.2011.647753>
- (6) M. Mileusnić, B.S. Mapani, A.F. Kamona, S. Ružićić, I. Mapaure and P.M. Chimwamurombe, Assessment of agricultural soil contamination by potentially toxic metals dispersed from improperly disposed tailings, Kombat mine, Namibia, *J. Geochem. Explor.*, 2014, **144**, 409–420. <https://doi.org/10.1016/j.gexplo.2014.01.009>
- (7) O. Sracek, M. Mihaljevič, B. Kříbek, V. Majer, J. Filip, A. Vaněk, V. Penížek, V. Ettler and B. Mapani, Geochemistry of mine tailings and behavior of arsenic at Kombat, northeastern Namibia, *Environ. Monit. Assess.*, 2014, **186**, 4891–4903. <https://doi.org/10.1007/s10661-014-3746-1>
- (8) M. Mihaljevič, R. Baieta, V. Ettler, A. Vaněk, B. Kříbek, V. Penížek, P. Drahota, J. Trubač, O. Sracek, V. Chrastný and B.S. Mapani, Tracing the metal dynamics in semi-arid soils near mine tailings using stable Cu and Pb isotopes, *Chem. Geol.*, 2019, **515**, 61–76. <https://doi.org/10.1016/j.chemgeo.2019.03.026>

- (9) V. Ettler, M. Cihlová, A. Jarošíková, M. Mihaljevič, P. Drahota, B. Kříbek, A. Vaněk, V. Penížek, O. Sracek, M. Klementová, Z. Engel, F. Kamona and B. Mapani, Oral bioaccessibility of metal(loid)s in dust materials from mining areas of northern Namibia. *Environ. Int.*, 2019, **124**, 205–215. <https://doi.org/10.1016/j.envint.2018.12.027>
- (10) J.E. Lee and D.A. Glenister, Stratiform sulfide mineralization at Oamites copper mine, South West Africa, *Econ. Geol.*, 1976, **71**, 369–383. <https://doi.org/10.2113/gsecongeo.71.1.369>
- (11) M.N. Uugwanga and N.A. Kgabi, Assessment of metals pollution in sediments and tailings of Klein Aub and Oamites mine sites, Namibia, *Environ. Adv.*, 2020, **2**, 100006. <https://doi.org/10.1016/j.envadv.2020.100006>
- (12) M.N. Uugwanga and N.A. Kgabi, Dilution and dispersion of particulate matter from abandoned mine sites to nearby communities in Namibia, *Heliyon*, 2021, **7**, e06643. <https://doi.org/10.1016/j.heliyon.2021.e06643>
- (13) L. Hahn, F. Solesbury and S. Mwiya, Report: Assessment of potential environmental impacts and rehabilitation of abandoned mine sites in Namibia, *Comm. Geol. Survey Namibia*, 2004, **13**, 85–91.
- (14) I. Hasheela, G.I.C. Schneider, R. Ellmies, A. Haidula, R. Leonard, K. Ndaluilwa, O. Shigwana and B. Walmsley, Risk assessment methodology for shut-down and abandoned mine sites in Namibia, *J. Geochem. Explor.*, 2014, **144**, 572–580. <https://doi.org/10.1016/j.gexplo.2014.05.009>
- (15) L.J. Basson, M.-J. McCall, J. Andrew and E. Daweti, Structural controls on mineralization at the Namib Lead and Zinc Mine, Damara Belt, Namibia, *Ore Geol. Rev.*, 2018, **95**, 931–944. <https://doi.org/10.1016/j.oregeorev.2018.03.028>
- (16) S. Lohmeier, D. Gallhofer and B.G. Lottermoser, Field-portable X-ray fluorescence analyzer for chemical characterization of carbonate-bearing base metal tailings: case study from Namib Pb-Zn Mine, Namibia. *J. Southern Afr. Inst. Mining Metall.*, 2024, **124**, 421–436. <https://doi.org/10.17159/2411-9717/2676/2024>
- (17) S. Lohmeier, D. Gallhofer and B.G. Lottermoser, Geochemical and mineralogical characterization and resource potential of the Namib Pb-Zn tailings (Erongo Region, Namibia), *J. Southern Afr. Inst. Mining Metall.*, 2024, **124**, 447–459. <https://doi.org/10.17159/2411-9717/2724/2024>
- (18) SW-846 Test Method 1340. *In Vitro Bioaccessibility Assay for Lead in Soil*. US EPA, Washington, 2017. <https://www.epa.gov/hw-sw846/sw-846-test-method-1340-vitro-bioaccessibility-assay-lead-soil>
- (19) M. Dodd, D. Lee, J. Nelson, S. Verenitch and R. Wilson, In vitro bioaccessibility round robin testing for arsenic and lead in standard reference materials and soil samples, *Integr. Environ. Assess. Manag.*, 2024, **20**, 1486–1495. <https://doi.org/10.1002/ieam.4891>
- (20) L.N. Warr, IMA-CNMNC approved mineral symbols, *Mineral. Mag.*, 2021, **85**, 291–320. <https://doi.org/10.1180/mgm.2021.43>
- (21) A. J. Baars, R.M.C. Theelen, P.J.C.M. Janssen, J.M. Hesse, M.E. van Apeldoorn, M.C.M. Meijerink, L. Verdam, M.J. Zeilmaker, *Re-evaluation of human-toxicological maximum permissible risk levels*, Bilthoven, the Netherlands: RIVM report 711701025, 2001.
- (22) B. Tiesjema, A.J. Baars, *Re-evaluation of some human-toxicological maximum permissible risk levels earlier evaluated in the period 1991–2001*, Bilthoven, the Netherlands: RIVM report 711701092, 2009
- (23) Minimal Risk Levels (MRLs). Agency for Toxic Substances and Disease Registry (ATSDR), February 2022. Atlanta, USA. <https://www.atsdr.cdc.gov/mrls/index.html>